Role of planet rotation on the onset of aquaplanet monsoon

Wen Shi, Liyuan Weng and Xueyang Zhang

Department of Earth System Science, Tsinghua University

ABSTRACT

Earth's rotation rate has changed significantly in history. An idealized GCM is used to investigate the effect of Earth's rotation rate on the monsoon of an aquaplanet with a shallow mixed layer. 0.25Ω, 0.5Ω, Ω, 2Ω and 4Ω are used in the simulations. Annual cycles of ITCZ precipitation and sea-level air temperature are shown, with further detailed information such as ITCZ migration rate and SST maximum. It is shown that although the major patterns of ITCZ annual cycle remain, some of the ITCZ migration manners differ. Meridional circulation shows abrupt shift before and after the aquaplanet monsoon accompanied by the change of the distribution of angular momentum, especially in the high rotation rate case.

1. Introduction

As one of the responses of the coupled atmosphere–land–ocean system to seasonal variation of the solar radiation forcing, monsoon brings climate characterized by wet summers and dry winters to its domain. The traditional view is that the monsoon is land-sea breeze caused by the difference in heat capacity between the ocean and land. It is defined by the seasonal change in the direction of the prevailing wind, with its domains located at Asia, Africa and Australia (Wang, 2010). However, several innovative ideas about the monsoon emerged since the late 20th century. First, rather than regional phenomena independent of each other, monsoons are more likely to be embedded with a global system characterized by the seasonal reversal of large-scale circulation (Trenberth et al., 2000). Second, compared to the prevailing wind, the concurrent heavy rainfall should be a more significant quantity to human due to its large impact on agriculture (Wang and Ding, 2008). Based on these two views, Wang and Ding (2008) distinguished "dry" and "wet" seasons based on the leading MV-EOF modes of low-level circulation together with precipitation at tropics, and define regions where precipitation is mainly concentrated in summer and exceeds a threshold as global monsoon domains. Six major monsoon domains are delineated including ocean regions.

In addition to these attempts to extend the concept of the monsoon in terms of spatial extent, it is believed that monsoon is closely linked to the surrounding large-scale circulation, including the major meridional overturning circulation in the tropics, i.e., the Hadley circulation. More specifically, some of the monsoon systems are closely linked to the upwelling branch of the Hadley circulation, commonly referred to as the ITCZ. For example, Gray (1968) found that the onset of western Pacific monsoon involves an abrupt northward shift of the ITCZ, and Chao (2000) explained this feature of the western Pacific monsoon in terms of the dynamics of the ITCZ with multiple quasi-equilibria. Gadgil (2003, 2018) argued that the Indian monsoon is the same system as a seasonal migrating ITCZ because of the similarity between the monsoon precipitation system and deep convections in ITCZ in terms of their vertical structure, as well as the similarity between seasonal migrating cloud belts over monsoonal India and oceanic ITCZ counterparts in their behavior.

Intuitively, ITCZ may tend to follow the insolation maximum, but it turns out that the observed zonal mean ITCZ undergoes an abrupt shift in spring and fall (Chiang and Friedman, 2012). Schneider et al. (2014) notes that the seasonal migration of the ITCZ behaves differently in different regions. Over Pacific, the seasonal migration of ITCZ is continuous and sinusoidal, with a moderate amplitude. In the South Asian monsoon sector, the migration is more like a square wave with large and abrupt shifts. Such abrupt shift of ITCZ is associated with sudden onset and retreat of monsoons, and it is also related to the nature of the meridional overturning circulation. Therefore, dynamics of seasonal varying Hadley circulation may also contribute to explain the abrupt onset of monsoon. It has long been observed that in winter and summer, the two Hadley cells are asymmetric with the winter Hadley cell much stronger than the one in the opposite summer hemisphere (Dima and Wallace, 2003), which is called a solstitial regime. In spring and autumn, the Hadley cells are in an equinoctial regime. When the subsolar point moves poleward from the equator, the Hadley cells are initially equinoctial, i.e., ITCZ is close to the equator, which is the state before the monsoon onset. Next, the Hadley cells switch to the solstitial regime, and in the meantime the upwelling branch of the winter Hadley circulation in the opposite hemisphere builds up and becomes stronger at a poleward latitude, which also means ITCZ abruptly shifts poleward and the monsoon outbreaks.

In order to explain some of the characteristics of monsoon by the dynamical theory about the Hadley circulation, a series of theories have been proposed, including the axisymmetric case and the eddy-permitting case. Aquaplanet experiments which can simulate some basic physics of the system are conducted to prove these theories, leading to the concept of Aquaplanet monsoon. The classical Held-Hou model (Held and Hou, 1980) of the Hadley circulation can explain the annual mean Hadley circulation, followed by Plumb and Hou (1992) to give a theoretical model under off-equatorial thermal forcing. Prive and Plumb (2007) further showed that under the assumptions of slantwise convective neutrality, the precipitation maximum is associated with ITCZ is related to low-level entropy or sub-cloud MSE, i.e., located at or slightly equatorward of the sub-cloud MSE maximum. As to the abrupt shift of ITCZ, Xian and Miller (2008) developed a model with a slab ocean and seasonal variation of solar radiation. It is moist adiabatic everywhere and eddies are excluded. They found that the abrupt shift of ITCZ requires a sufficiently low ocean heat capacity, and that the advection of angular momentum by meridional circulation is critical for this process. Above are all axisymmetric models, and Bordoni and Schneider (2008) later introduced the role of eddy and found that the equinoctial Hadley cell does not conserve its angular momentum in the upper branch due to the influence of eddy momentum transport in the subtropics, while the solstitial Hadley cell is AM-conserving. It can be explained that the switch of the Hadley circulation between the two regimes is "mediated" by eddies.

Whether the Hadley cell conserves its angular momentum is theoretically dependent on the Rossby number, Ro (2008), which indicates that the Earth's rotation rate may be critical for the theoretical study of ITCZ migration dynamics. Both theory and aquaplanet experiments have demonstrated that the maximum boundary of a solstitial Hadley cell (SHC) or the northernmost ITCZ can reach will increase with decreasing Earth's rotation rate (Faulk et al., 2017; Gill, 1980; Singh, 2019). These studies are extreme cases with the maximum solar insulation located at the pole. Back to the nonlinear seasonal migration behavior of ITCZ, Geen et al. (2018, 2019, 2020) continue the eddy-permitting and moist aquaplanet experiment, exploring the effects of several factors including the extent of zonal-symmetric-distributed land, the annual period, Earth's rotation rate, etc. Among the interesting findings are that the latitude at which ITCZ begins to migrate abruptly, which is called transition latitude, does not vary with the annual period or equivalent ocean mix layer depth, and that the maximum migration rate changes non-monotonically with Earth's rotation rate, being fastest at the actual Earth's rotation rate (Geen et al., 2019). It seems that the Earth is tuned for a fast ITCZ migration. Our term paper further looks into this non-monotonic behavior as there have been no quantitative analysis of it

2. Method

a. Model and experiments

We use “Isca”, a framework to set up idealized GCMs, to simulate atmosphere circulation under different Earth’s rotation rates. This framework is based on the GFDL Flexible Modeling System with a variety of radiation, convection, continent, surface process and astronomical parameter options. Due to its flexibility, it is easy to set up models with varying levels of complexity for earth and exoplanets. For more information, refer to Vallis et al. (2018).

For the control case (referred as ctrl hereafter), the setup is as in Geen et al. (2018).A slab ocean of 2m mixed layer depth without Q fluxes is adopted in the model, coupled with the Rapid Radiative Transfer Model (Mlawer et al., 1997) with timestep set to 3600 seconds, which means that it runs every 5 atmospheric timesteps, and the simplified Betts-Miller scheme(Betts, 1986; Betts & Miller, 1986). No clouds are included. The horizontal resolution is T42 and the number of vertical layers is 40. Apart from the control case, the simulations are performed under four rotation rates: 4 times larger, 2 times larger, 2 times smaller and 4 times smaller than Earth’s value, referred as f4, f2, s2 and s4 respectively hereafter. All the other parameters are same.

All simulations are run for 32 years from an initial state of 285K. Spin-up periods are decided according to the tropical mean surface temperature (Fig. 1), which undergo an increase during spin-up periods and steady annual cycles afterwards. Therefore, values for the f4 simulation are averaged over the last 20 years (12 years of spin-up) while values for the other four simulations are averaged over the last 26 years (6 years of spin-up).

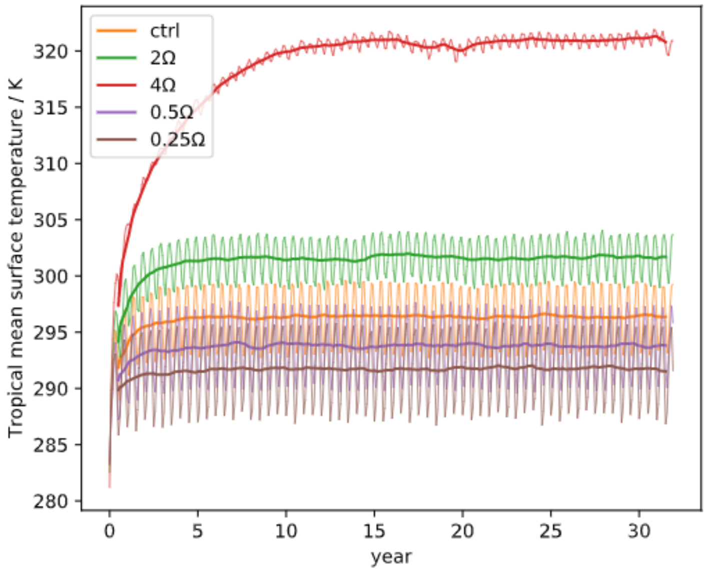

Figure 1. Time series of tropical mean surface temperature during the whole run (temperature are averaged between 30°S~30°N)

b. Data processing

Two metrics that have been used to define the ITCZ location based on precipitation are the maximum (Kang et al., 2008) and the centroid of tropical precipitation (Frierson and Hwang, 2012), where the latitude range of tropical region is defined as 15°S-15°N. In our experiments, the latitude of precipitation varies greatly as the Earth rotation rate changes, and the underlying boundary condition also deviates from a realistic one. Therefore, it is necessary to determine a latitude range (shown in Table 1) for calculation based the location of tropical precipitation in each experiment to avoid the disturbance of mid-latitude.

The precipitation centroid, defined as

$$\phi_{ITCZ} = \frac{\int_{\phi_1}^{\phi_2} \phi' P(\phi') \cos(\phi') \mathrm{d}\,\phi'}{\int_{\phi_1}^{\phi_2} P(\phi') \cos(\phi') \mathrm{d}\,\phi'},$$

is chosen because it appears smoother than the maximum line (Fig. 3), less disturbed by noises in our simulation results. However, the precipitation centroid is still affected by non-ITCZ precipitation, so we further choose precipitation exceeding 8mm/day for calculation. As shown in Fig. 3, this precipitation centroid fits migrating ITCZ well even in the rapid shift period.

Geen et al. (2019) chose a latitude range of 45°S~45°N for all experiments and did not mention whether a precipitation threshold is set. Therefore, the calculation of the maximum migration rate may be inaccurate in experiments where the Earth's rotation rate varies, leading to the necessity to double-check the conclusion of non-monotonic behavior.

Experiment	Latitude range for precipitation centroid calculation	Days selected for circulation comparison	
		Before onset	After onset
ctrl	40°S~40°N	156~165	216~225
f2	30°S~30°N	176~185	241~250
f4	15°S~15°N	191~200	226~245
s2	55°S~55°N	146~155	191~200
s4	90°S~90°N	126~135	191~200

Table 1. Spatial or temporal selection for data processing of each experiment

The angular momentum of tropical atmosphere is calculated as:

$$M = \Omega a^2 \cos^2\phi + ua\cos\phi,$$

where Ω is Earth's rotation rate, a is radius of Earth, u means zonal wind and ϕ means latitude. The streamfunction of zonal mean meridional overturning circulation is calculated as:

$$\Psi(\phi, p) = \frac{2\pi a\cos\phi}{g}\int_0^p [\overline{v}(p')]dp',$$

where [ ] denotes zonal mean and overbar denotes temporal mean during certain period. g is the gravity acceleration and v means meridional wind. Eddy momentum flux is $\nabla \cdot ([\overline{u'\boldsymbol{v}'}]\cos\phi)$. Here $u' = u - [\overline{u}]$ and $[\overline{u}]$ means zonal mean and temporal mean over 21 days around this data points, i.e., a 21-day running mean. The divergence of any vector F in spherical coordinate can be calculated as:

$$(\nabla \cdot F)_\phi = \frac{1}{r_0\cos\phi}\frac{\partial}{\partial\phi}(F_\phi\cos\phi),$$

where the subscript ϕ means the latitudinal component of this vector.

3. Results

a. precipitation and ITCZ migration

Figure 2 shows the seasonal cycle of precipitation and SAT for the 5 experiments. We use the precipitation centroid, which is defined as the latitude that is the centroid of the area-integrated tropical precipitation, as an evaluation of the ITCZ location. The integrated range of latitudes is specifically chosen to exclude non-ITCZ precipitation in each experiment. Generally, the ITCZ and precipitation distribution resembles a time-asymmetric sinusoid. The ITCZ exhibits a relatively faster migration poleward and a relatively slower migration equatorward. This ITCZ migration asymmetry is most evident in the f4 experiment, with the ITCZ almost stagnant in the subtropics after the monsoon onset. The one exception is in the s4 experiment, where the poleward and equatorward ITCZ migration rate are very close. Therefore, we can conclude that the asymmetry between monsoon onset and retreat becomes more significant with increasing rotation rate. The precipitation distribution shows a similar time-asymmetry as the ITCZ migration rate, with heavier precipitation migrating poleward and lighter precipitation migrating equatorward. It is noticeable that in the f4 experiment there exists strong extratropical precipitation in the winter hemisphere, while in all other experiments no significant winter extratropical precipitation is observed. In the control experiment, from pentad 37 to 42, the abrupt rapidity of ITCZ migration and sudden intensification of precipitation in Northern Hemisphere mark the monsoon onset and a transition from the equinoctial regime to the solstitial regime. During the monsoon retreat, the ITCZ migrates gradually equatorward with relatively slight precipitation, followed by the next monsoon onset from pentad 1 to 6 in Southern Hemisphere.

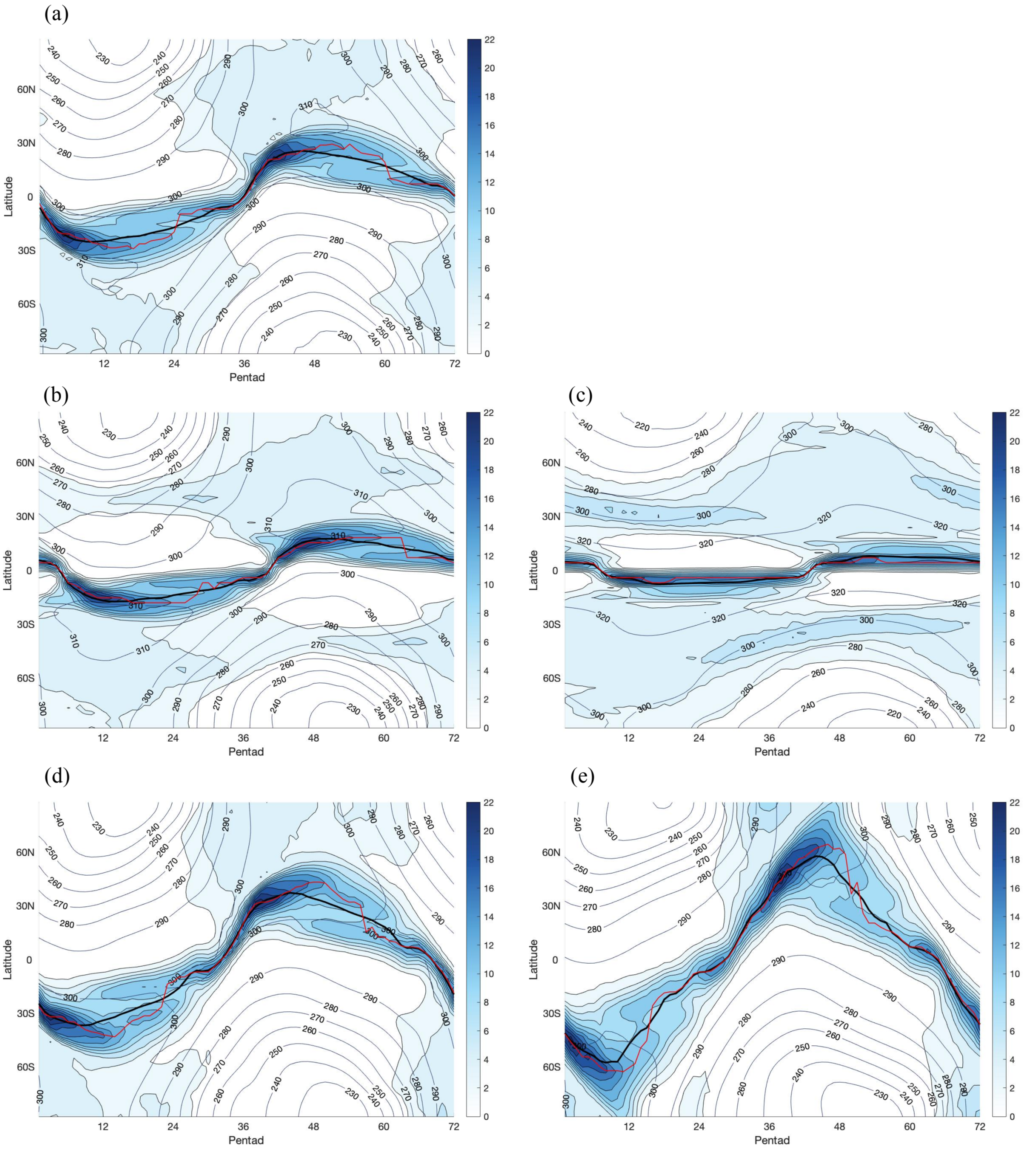

Figure 2. Seasonal cycle of zonal-mean and pentad-mean precipitation (color contours, mm day $^{-1}$) and sea-level air temperature (SAT; black contours with labels, K) for the (a) control, (b) f2, (c) f4, (d) s2, (e) s4 experiments. The precipitation centroid is indicated by the black line, and the latitude of maximum precipitation is indicated by the red line.

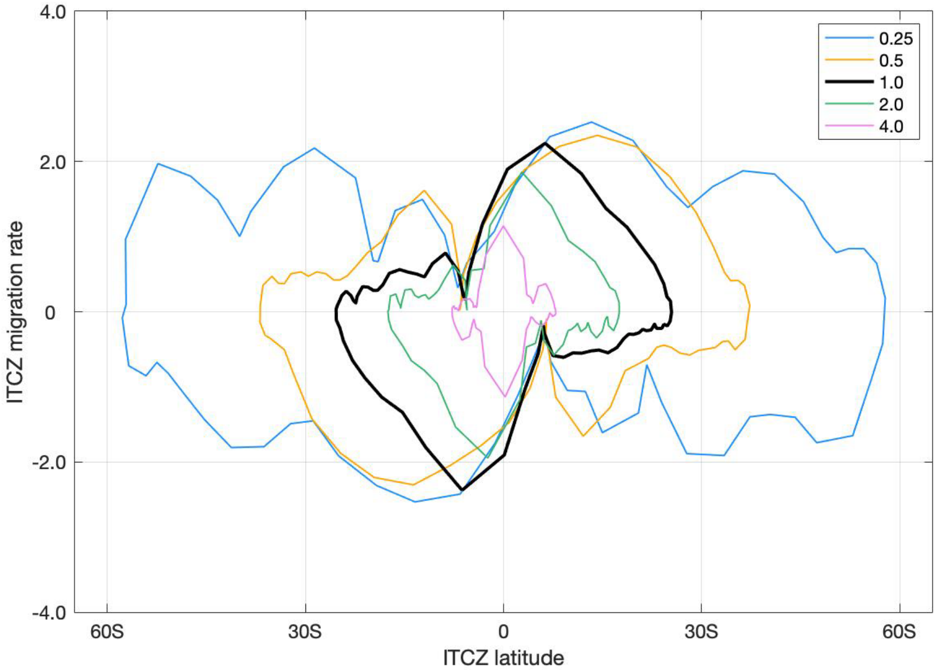

Figure 3. Precipitation centroid (°) versus rate of migration of the precipitation centroid (°day^{-1}) calculated from zonal-mean and pentad-mean precipitation. The control experiment is indicated by the heavy black line.

Figure 3 shows the trajectory of precipitation centroid vs migration rate of the precipitation centroid. If the ITCZ latitude is a perfect sinusoid, like the subsolar point, the closed trajectory in the latitude vs migration rate space would be expected to be an ellipse. Therefore, any deviations of the trajectory from an ellipse indicate deviations of the ITCZ displacement from a sinusoidal oscillator with time. In Fig 3, 5 closed trajectories in different experiments are shown. It is very interesting to see that all 5 experiments exhibit the abrupt shift of ITCZ, with a poleward migration rate minimum followed by a sudden migration rate maximum, which marks the monsoon onset. The maximum latitude that ITCZ can reach decreases with increasing rotation rate, which is sensible as the model has less time to equilibrate, while the location of maximum migration rate moves equatorward with increasing rotation rate. Regrettably, the relation of maximum migration rate and planetary rotation rate is unclear, for the maximum rate in control, s2 and s4 experiments are too close to produce a robust conclusion. This problem may be solvable if we run more ensembles and adjust our experiment settings in the future research.

(a) (b)

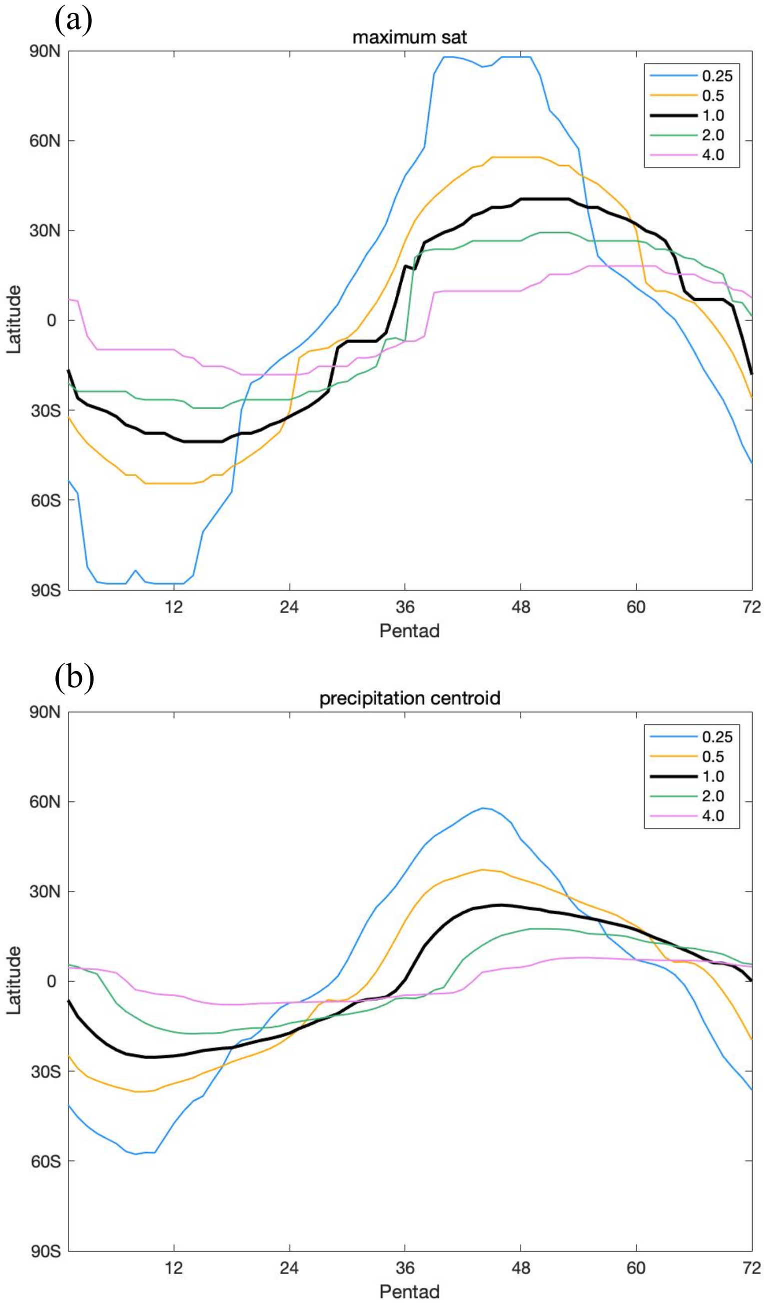

Figure 4. (a) Seasonal cycle of latitude of maximum sea-level air temperature (SAT). (b) Seasonal cycle of the precipitation centroid (°). All are calculated from zonal-mean and pentad-mean precipitation.

Figure 4 shows the seasonal cycle of the latitude of maximum SAT and precipitation centroid. The latitude of maximum sea-level air temperature and the ITCZ (indicated by the precipitation centroid) are not in phase with the subsolar point. Take the control experiment (black bold line) as an example, at around pentad 36 the subpolar point is near the summer solstice, while maximum SAT and ITCZ locate close to the equator. The precipitation centroid is in phase with the latitude of maximum SAT, both lagging the movement of subsolar point. The phase lag increases with increasing planetary rotation rate, from around $\pi/6$ in the s4 experiment to around $2\pi/3$ in the f4 experiment. Considering the small thermal surface inertia in the experiment, we cannot find a reasonable explanation for the existence of this phase lag so far. Generally, the latitude of maximum SAT moves more poleward than ITCZ, with the latitude of maximum SAT reaching nearly $90°$ in s4 experiment, another point remains under discussion. Both the latitude of maximum SAT and ITCZ moves poleward with decreasing rotation rate, consistent with the conclusion that Hadley cell expands with longer rotation period in Geen et al. (2019). The gap between maximum SAT location and ITCZ becomes smaller with increasing rotation rate, meaning that the ITCZ tends to follow maximum SAT location if the planet rotates fast enough.

b. eddy momentum flux

Figure 5 shows the meridional overturning circulation, angular momentum and divergence of eddy momentum flux before and after the monsoon onset. Days selected for plotting is shown in Table 1. Before the monsoon onset, there exists two Hadley cells with comparable strength, almost symmetric about the equator, which is referred to as the equinoctial regime. After the onset, the circulation shifts to the solstitial regime, dominated by a very strong cross-equatorial winter cell, with upward motion in the summer hemisphere subtropics. If the overturning circulation conserves angular momentum, streamlines and angular momentum contours should coincide. Therefore, large deviations from angular momentum conservation occur where the circulation streamlines cross angular momentum contours, indicating the strong effects of eddy. The reason why the divergence of eddy momentum flux is stronger after onset than before onset is still unclear and remains to be further discussed. It should be noted that the angular momentum contours in the f4 experiment looks very different from other experiments, so are the vertical location of eddy momentum flux. The reason is that in the f4 experiment, the tilting of angular momentum contours and the location of eddy momentum flux are at a higher vertical level, which is squeezed in the linear pressure coordinate.

Figure 6 shows zonal-mean zonal wind and divergence of eddy momentum flux before and after the monsoon onset. Important dynamical feedback mechanisms act during the regime change of meridional overturning circulation, leading to the rapidity of circulation regime change relative to radiative heating. As the cross-equatorial cell develops, easterlies develop and extend in the upper branch. The upper-level easterlies shield the cross-equatorial cell from strong eddy momentum fluxes, which are mostly limited to the location of westerlies. The surface zonal wind undergoes a direction change in the summer hemisphere subtropics, being easterlies before the onset and westerlies in the monsoon regime. The advection of cold air by the lower branch of the cross-equatorial winter cell leads to the poleward movement of the ascending center and the strengthening and extension of the cross-equatorial cell.

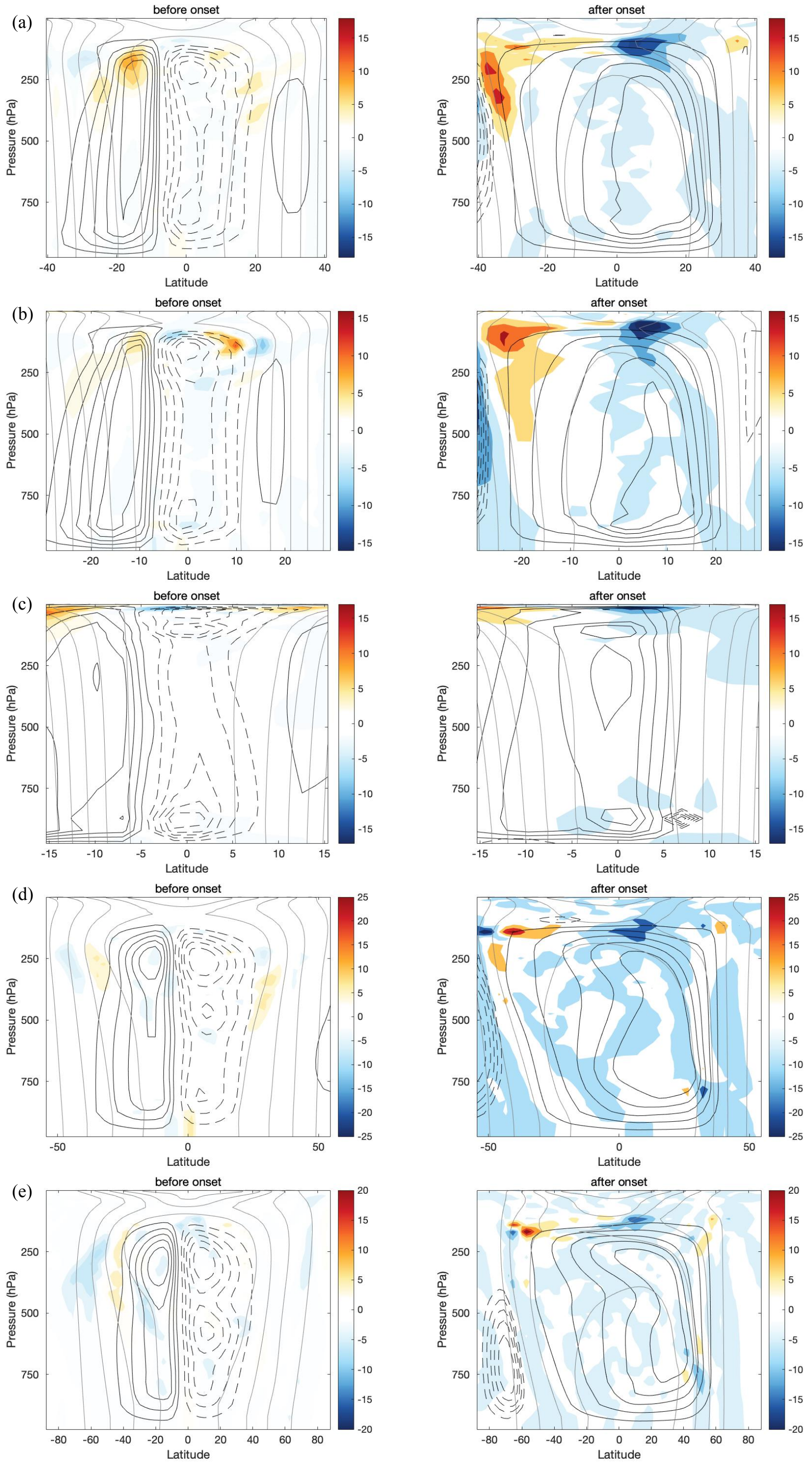

Figure 5. Zonal-mean and temporal-mean circulation at 10-day period before (left panels) and after (right panels) monsoon onset for the (a) control, (b) f2, (c) f4, (d) s2, (e) s4 experiments. Streamfunction of meridional overturning circulation (black contours, with solid contours for anticlockwise rotation and dashed contours for clockwise rotation), angular momentum per unit mass (grey contours, scaled by $\Omega a^2/15$ with planetary rotation rate Ω and radius a) and transient eddy momentum flux divergence (color contours, with red tones for positive and blue tones for negative values).

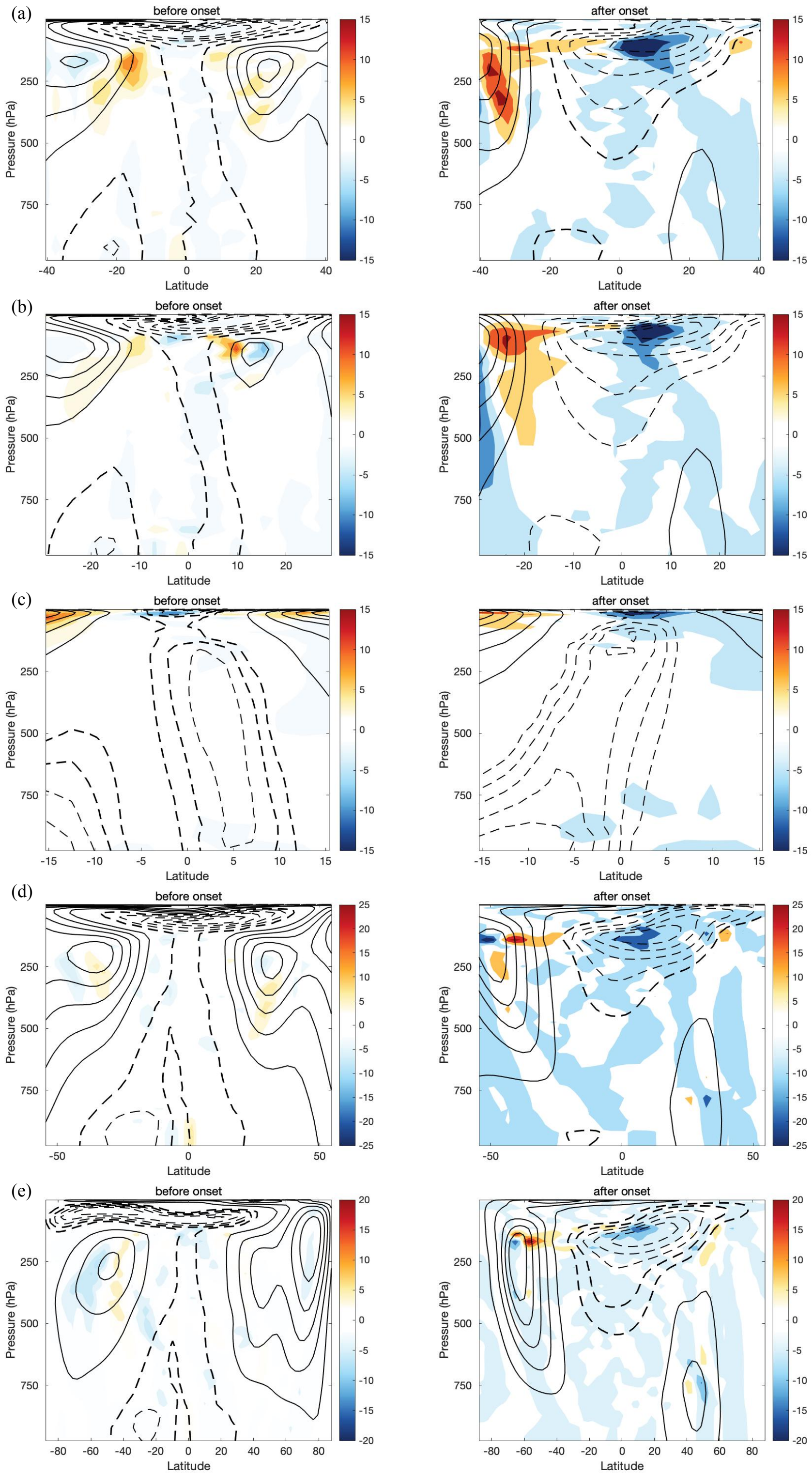

Figure 6. Zonal-mean and temporal-mean circulation at 10-day period before (left panels) and after (right panels) monsoon onset for the (a) control, (b) f2, (c) f4, (d) s2, (e) s4 experiments. Zonal wind (black contours, with solid contours for westerlies and dashed contours for easterlies) and transient eddy momentum flux divergence (color contours, with red tones for positive and blue tones for negative values).

4. Summary and discussion

Following a series of previous studies on the aquaplanet monsoon, we conduct idealized experiments with shallow slab ocean and annual variations to investigate the effect of Earth's rotation rate on the aquaplanet monsoon. Annual cycles of ITCZ precipitation and SAT are plotted, with further detailed information such as ITCZ migration rate and SST maximum subsequently calculated. As Earth's rotation rate varies, although the major patterns of ITCZ annual cycle, e.g., temporal asymmetry during onset and retreat, still remain, some of the ITCZ migration manner in extreme conditions deviates the control results. Meridional sections before and after the aquaplanet monsoon are also shown with different Earth's rotation rates.

The non-monotonic behavior in Geen et al. (2019) is not replicated in our experiments. It is mainly because of the relationship between maximum migration rate and Earth's rotation rate is not robust for slow rotation experiments. The definition of ITCZ position in this paper differs from that in Geen et al. (2019), but fits migrating ITCZ well Earth's rotation rate varies. The non-robustness may arise from the fact that experiments are not long enough and the climatology data contains some noises.

In the future, we would further show the annual cycle of meridional streamfunction and sub-cloud MSE with a range of Earth's rotation rates. We also hope to estimate the Rossby number of the upper-level branch of Hadley circulation, using theories in Bordoni and Schneider (2008) to assess the effect of eddies on the circulation regimes, so that we can analyze it from a dynamical point of view with current models

REFERENCES

Betts, A. K. (1986). A new convective adjustment scheme. Part I: Observational and theoretical basis. *Quarterly Journal of the Royal Meteorological Society*, *112*(473), 677–691. https://doi.org/10.1002/qj.49711247307

Betts, A. K., & Miller, M. J. (1986). A new convective adjustment scheme. Part II: Single column tests using GATE wave, BOMEX, ATEX and arctic air-mass data sets. *Quarterly Journal of the Royal Meteorological Society*, *112*(473), 693–709. https://doi.org/10.1002/qj.49711247308

Bordoni, S., & Schneider, T. (2008). Monsoons as eddy-mediated regime transitions of the tropical overturning circulation. *Nature Geoscience*, *1*(8), 515–519. https://doi.org/10.1038/ngeo248

Chao, W. C. (2000). Multiple Quasi Equilibria of the ITCZ and the Origin of Monsoon Onset. *JOURNAL OF THE ATMOSPHERIC SCIENCES*, *57*, 11.

Chiang, J. C. H., & Friedman, A. R. (2012). Extratropical Cooling, Interhemispheric Thermal Gradients, and Tropical Climate Change. *Annual Review of Earth and Planetary Sciences*, *40*(1), 383–412. https://doi.org/10.1146/annurev-earth-042711-105545

Dima, I. M., & Wallace, J. M. (2003). On the Seasonality of the Hadley Cell. *Journal of Atmospheric Sciences*, *60*(12), 1522–1527. https://doi.org/10.1175/1520-0469(2003)060<1522:OTSOTH>2.0.CO;2

Faulk, S., Mitchell, J., & Bordoni, S. (2017). Effects of Rotation Rate and Seasonal Forcing on the ITCZ Extent in Planetary Atmospheres. *JOURNAL OF THE ATMOSPHERIC SCIENCES*, *74*, 14.

Frierson, D. M. W., & Hwang, Y.-T. (2012). Extratropical Influence on ITCZ Shifts in Slab Ocean Simulations of Global Warming. *Journal of Climate*, *25*(2), 720–733. https://doi.org/10.1175/JCLI-D-11-00116.1

Gadgil, S. (2003). The Indian monsoon and its variability. *Annual Review of Earth and Planetary Sciences*, *31*(1), 429–467. https://doi.org/10.1146/annurev.earth.31.100901.141251

Gadgil, S. (2018). The monsoon system: Land-sea breeze or the ITCZ? *Journal of Earth System Science*, *127*, 1. https://doi.org/10.1007/s12040-017-0916-x

Geen, R., Bordoni, S., Battisti, D. S., & Hui, K. (2020). Monsoons, ITCZs and the Concept of the Global Monsoon. *Reviews of Geophysics*. https://doi.org/10.1029/2020RG000700

Geen, R., Lambert, F. H., & Vallis, G. K. (2018). Regime Change Behavior during Asian Monsoon Onset. *Journal of Climate*, *31*(8), 3327–3348. https://doi.org/10.1175/JCLI-D-17-0118.1

Geen, R., Lambert, F. H., & Vallis, G. K. (2019). Processes and Timescales in Onset and Withdrawal of '"Aquaplanet Monsoons."' *JOURNAL OF THE ATMOSPHERIC SCIENCES*, *76*, 17.

Gill, A. E. (1980). Some simple solutions for heat-induced tropical circulation. *Quarterly Journal of the Royal Meteorological Society*, *106*(449), 447–462. https://doi.org/10.1002/qj.49710644905

Gray, W. M. (1968). GLOBAL VIEW OF THE ORIGIN OF TROPICAL DISTURBANCES AND STORMS. *Monthly Weather Review*, *96*(10), 669–700. https://doi.org/10.1175/1520-0493(1968)096<0669:GVOTOO>2.0.CO;2

Held, I. M., & Hou, A. Y. (1980). Nonlinear Axially Symmetric Circulations in a Nearly Inviscid Atmosphere. *Journal of Atmospheric Sciences*, *37*(3), 515–533. https://doi.org/10.1175/1520-0469(1980)037<0515:NASCIA>2.0.CO;2

Kang, S. M., Held, I. M., Frierson, D. M. W., & Zhao, M. (2008). The Response of the ITCZ to Extratropical Thermal Forcing: Idealized Slab-Ocean Experiments with a GCM. *Journal of Climate*, *21*(14), 3521–3532. https://doi.org/10.1175/2007JCLI2146.1

Mlawer, E. J., Taubman, S. J., Brown, P. D., Iacono, M. J., & Clough, S. A. (1997). Radiative transfer for inhomogeneous atmospheres: RRTM, a validated correlated-k model for the longwave. *Journal of Geophysical Research: Atmospheres*, *102*(D14), 16663–16682. https://doi.org/10.1029/97JD00237

Plumb, R. A., & Hou, A. Y. (1992). The Response of a Zonally Symmetric Atmosphere to Subtropical Thermal Forcing: Threshold Behavior. *Journal of Atmospheric Sciences*, *49*(19), 1790–1799. https://doi.org/10.1175/1520-0469(1992)049<1790:TROAZS>2.0.CO;2

Privé, N. C., & Plumb, R. A. (2007). Monsoon Dynamics with Interactive Forcing. Part I: Axisymmetric Studies. *Journal of the Atmospheric Sciences*, *64*(5), 1417–1430. https://doi.org/10.1175/JAS3916.1

Schneider, T., Bischoff, T., & Haug, G. H. (2014). Migrations and dynamics of the intertropical convergence zone. *Nature*, *513*(7516), 45–53. https://doi.org/10.1038/nature13636

Singh, M. S. (2019). Limits on the Extent of the Solsticial Hadley Cell: The Role of Planetary Rotation. *Journal of the Atmospheric Sciences*, *76*(7), 1989–2004. https://doi.org/10.1175/JAS-D-18-0341.1

Trenberth, K. E., Stepaniak, D. P., & Caron, J. M. (2000). The Global Monsoon as Seen through the Divergent Atmospheric Circulation. *JOURNAL OF CLIMATE*, *13*, 25.

Vallis, G. K., Colyer, G., Geen, R., Gerber, E., Jucker, M., Maher, P., Paterson, A., Pietschnig, M., Penn, J., & Thomson, S. I. (2018). Isca, v1.0: A framework for the global modelling of the atmospheres of Earth and other planets at varying levels of complexity. *Geoscientific Model Development*, *11*(3), 843–859. https://doi.org/10.5194/gmd-11-843-2018

Wang, B., & Ding, Q. (2008). Global monsoon: Dominant mode of annual variation in the tropics. *Dynamics of Atmospheres and Oceans*, *44*(3–4), 165–183. https://doi.org/10.1016/j.dynatmoce.2007.05.002

Wang, S. (2010). *Global Monsoon*. *6*(6), 473–474.

Xian, P., & Miller, R. L. (2008). Abrupt Seasonal Migration of the ITCZ into the Summer Hemisphere. *Journal of Atmospheric Sciences*, *65*(6), 1878–1895. https://doi.org/10.1175/2007JAS2367.1